Deactivation Behavior and Excited-State Properties of (Coumarin-4-yl)methyl Derivatives. 1. Photocleavage of (7-Methoxycoumarin-4-yl)methyl-Caged Acids with Fluorescence Enhancement

Björn Schade,[†] Volker Hagen,[†] Reinhard Schmidt,[‡] Ralph Herbrich,[‡] Eberhard Krause,[†] Torsten Eckardt,[†] and Jürgen Bendig*,[§]

Research Institute of Molecular Pharmacology, Alfred-Kowalke-Strasse 4, D-10315 Berlin, Germany, Institute of Physical and Theoretical Chemistry, Johann-Wolfgang-Goethe University Frankfurt/Main, D-60439 Frankfurt/Main, Germany, and Institute of Chemistry, Humboldt University Berlin, Hessische Strasse 1−2, D-10115 Berlin, Germany

Received June 28, 1999

The photochemistry of the (7-methoxycoumarin-4-yl)methyl (MCM) carboxylates **3a**−**d**, the mesylate **4**, and the phosphates **5a**−**e** has been examined under near physiological conditions in acetonitrile or methanol/aqueous HEPES buffer solution, respectively. Analysis of photoproducts as well as measurements of photochemical quantum yields, fluorescence quantum yields, and lifetimes for the excited singlet state verified the similar photochemical and photophysical behavior of all the esters studied here. 4-(Hydroxymethyl)-7-methoxycoumarin (**2**) and the corresponding free acids were obtained as major products upon irradiation. The rates of deactivation of the excited MCM derivatives **3a**−**5e** were found to be dependent on the leaving group ability of the anion concerned as well as on the solvent polarity. The polarity dependence and the exclusive formation of ^{18}O-labeled **2** during irradiation of **5a** in ^{18}O-labeled water indicate that photocleavage of the excited singlet state of the MCM *caged* compounds **3a**−**5e** proceeds via a photo S_N1 mechanism (solvent-assisted photoheterolysis).

Introduction

The liberation of bioactive effector molecules from their photosensitive precursors (*caged* derivatives) is an attractive method which is used to an increasing extent for studies of the functionality and action of biomolecules inside living cells.[1,2] Since the photolytic cleavage of such precursors can be both temporally (short generating pulses) and spatially controlled, it is possible to trigger the biological response with almost no delay. The response can be analyzed by procedures such as immunological, electrophysiological, or imaging techniques. Especially for the latter method, the use of caging (protecting) groups leading to highly fluorescent products during the photolytic liberation of the biomolecule is particularly favorable. The release of such fluorescent photoproducts should offer the possibility of monitoring the phototriggering reaction and additionally, in combination with fluorescence microscopic procedures, to estimate the rate of photolysis and/or the concentration and local distribution of the liberated biomolecule.

Among the numerous caging groups[3] described until now the (7-methoxycoumarin-4-yl)methyl (MCM) caging group fulfills the requirement to a high degree. It was shown that the MCM moiety is favorable for the caging of phosphates, i.e., of adenosine cyclic-3′,5′-monophosphate (cAMP)[4] and guanosine cyclic-3′,5′-monophosphate (cGMP), as well as their derivatives. The main advantages of these *caged* compounds are their high photoefficiencies and hydrolytic stabilities. Several photochemical studies of such MCM esters of cGMP and cAMP[4] indicate that the efficiency of photocleavage, and therefore the liberation of the second messenger molecule, depends on the structure of the *caged* cyclic nucleotide as well as on the environment (especially the solvent polarity).

Recent investigations have focused on the photochemistry of 1-naphthylalkyl[5] and benzyl[6] derivatives. In these cases a heterolytic bond cleavage or a competition between homolytic versus heterolytic cleavage were respectively proposed.[4,7] However, there has previously been no mechanistic study describing the photolytic pathway of MCM derivatives. The question of whether a

* Corresponding author. E-mail: juergen=bendig@chemie.hu-berlin.de.
[†] Research Institute of Molecular Pharmacology.
[‡] Johann-Wolfgang-Goethe University Frankfurt/Main.
[§] Humboldt University Berlin.

(1) (a) Corrie, J. E. T.; Trentham, D. R. In *Bioorganic Photochemistry*; Morrison, H., Ed.; Wiley: New York, 1993; Vol. 2, pp 243−305. (b) Adams, S. R.; Tsien, R. Y. *Annu. Rev. Physiol.* **1993**, *55*, 755−784. (c) McCray, J. A.; Trentham, D. R.; *Annu. Rev. Biophys. Biophys. Chem.* **1989**, *18*, 239−270.

(2) (a) Hagen, V.; Dzeja, C.; Bendig, J.; Baeger, I.; Kaupp, U. B. *J. Photochem. Photobiol. B: Biol.* **1997**, *42*, 71−78. (b) Hagen, V.; Dzeja, C.; Frings, S.; Bendig, J.; Krause, E.; Kaupp, U. B. *Biochemistry* **1996**, *35*, 7762−7771.

(3) For reviews see: (a) Pillai, V. N. R. *Org. Photochem.* **1987**, *9*, 225−323. (b) Pillai, V. N. R. *Synthesis* **1980**, 1−26.

(4) (a) Furuta, T.; Torigai, H.; Sugimoto, M.; Iwamura, M. *J. Org. Chem.* **1995**, *60*, 3953−3956. (b) Bendig, J.; Helm, S.; Hagen, V. *J. Fluoresc.* **1997**, *7*, 357−361. (c) Furuta, T.; Iwamura, M. Caged Compounds. In *Methods of Enzymology*; Marriott, G., Ed.; Academic Press: San Diego, CA, 1998; Vol. 291, pp 50−63.

(5) (a) Itoh, Y.; Gouki, M.; Goshima, T.; Hachimori, A.; Kojima, M.; Karatsu, T. *J. Photochem. Photobiol. A* **1998**, *117*, 91. (b) Pincock, J. A. *Acc. Chem. Res.* **1997**, *30*, 43. (c) Arnold, B.; Donald, L.; Jurgens, A.; Pincock, J. A. *Can. J. Chem.* **1985**, *63*, 3140.

(6) Hilborn, J. W.; MacKnight, E.; Pincock, J. A.; Wedge, P. J. *J. Am. Chem. Soc.* **1994**, *116*, 3337.

(7) Givens, R. S.; Matuszewski, B. *J. Am. Chem. Soc.* **1984**, *106*, 6860−6861.

10.1021/jo9910233 CCC: $18.00
Published on Web 11/12/1999

Scheme 1. Pathways of the Photolytic Cleavage of MCM Derivatives: (a) Solvent-Assisted Photoheterolytic Cleavage with Ion Pair Formation; (b) Photosolvolysis Reaction

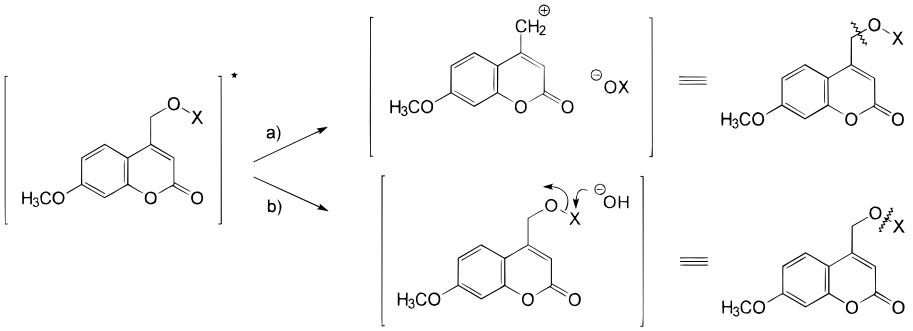

Scheme 2. Investigated MCM Caged Compounds

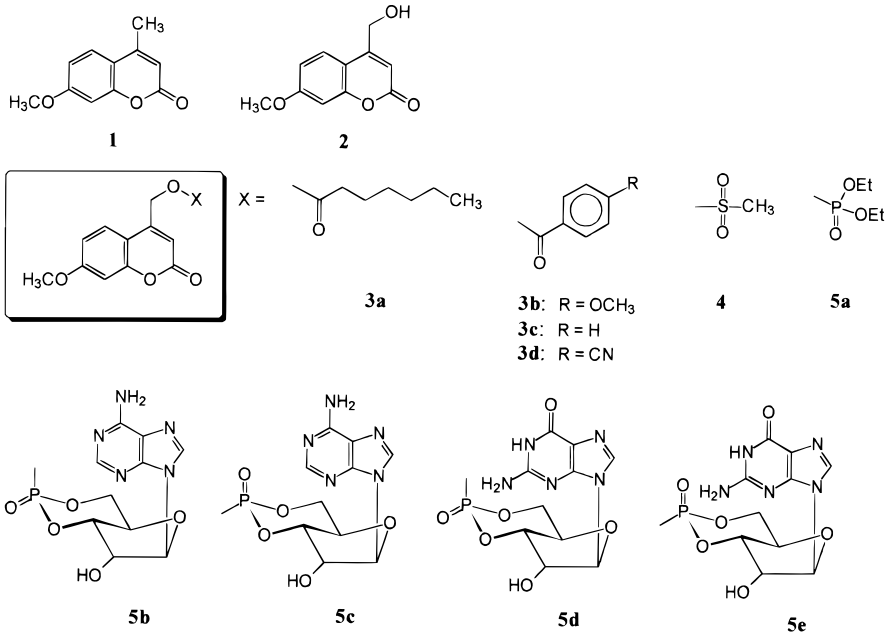

photo S_N1 reaction (solvent-assisted photoheterolysis, Scheme 1a) or of a photosolvolysis (Scheme 1b), characterized by a nucleophilic attack of the solvent at the C═O−, P═O−, or S═O center in the primary step, is involved remained unclear. Additionally, the deactivation behavior of the excited MCM *caged* compounds is characterized by the competition of photophysical and photochemical processes.[4] The understanding of the solvent influence on the efficiency of the photoreaction is rendered more difficult by the fact that the photophysical deactivation behavior of MCM derivatives, in terms of fluorescence quantum yields and lifetimes, already shows a distinctive solvent dependence in general.[8] The more complex solvent influence observed experimentally is presumed, therefore, to be a superimposition of two independent relationships.

We are currently investigating the suitability of the MCM caging group for the deactivation of biologically active substrates with different chemical functional groups. In the present paper we report the photochemical and photophysical deactivation behavior of MCM-protected model compounds and of the MCM-*caged* biomolecules cAMP and cGMP (Scheme 2). To investigate the structural influence on photochemistry, on a possible fluorescence enhancement, and on the rate of cleavage during photolysis a series of photolabile (7-methoxycoumarin-4-yl)methyl (MCM) derivatives was prepared and examined (Scheme 2, compounds **3a**−**5e**). Starting with the basic chromophore **1** and the photoproduct **2**, a systematic variation of the ester moiety was effected from the carboxylates **3a**−**d** via the phosphates **5a**−**e** to the mesylate **4**. A reaction pathway is proposed concerning the photolytic cleavage of MCM derivatives.

Results and Discussion

Synthesis of MCM Derivatives. 4-(Hydroxymethyl)-7-methoxycoumarin (**2**), a reference substance for analytical HPLC and fluorescence measurements, was prepared according to Sehgal and Seshadri[9] via hydrolysis of MCM acetate formed from **6** by refluxing in acetanhydride/sodium acetate (Scheme 3a). The MCM carboxylic acid esters **3a**−**d** were synthesized using a procedure described by Wilcox et al.[10] starting from **6** and the free carboxylic acids activated by potassium fluoride. This very mild and neutral method was chosen in order to retain the possibility of converting more sensitive car-

(8) Seixas de Melo, J. S.; Becker, R. S.; Macanita, A. L. *J. Phys. Chem.* **1994**, *98*, 6054−6058.

(9) Sehgal, J. M.; Seshadri, T. R. *J. Sci. Ind. Res.* **1953**, *12B*, 346.

(10) Wilcox, M.; Viola, R. W.; Johnson, K. W.; Billington, A. P.; Carpenter, B. K.; McCray, J. A.; Guzikowski, A. P.; Hess, G. P. *J. Org. Chem.* **1990**, *55*, 1585−1589.

Scheme 3. Synthesis of MCM Derivatives[a]

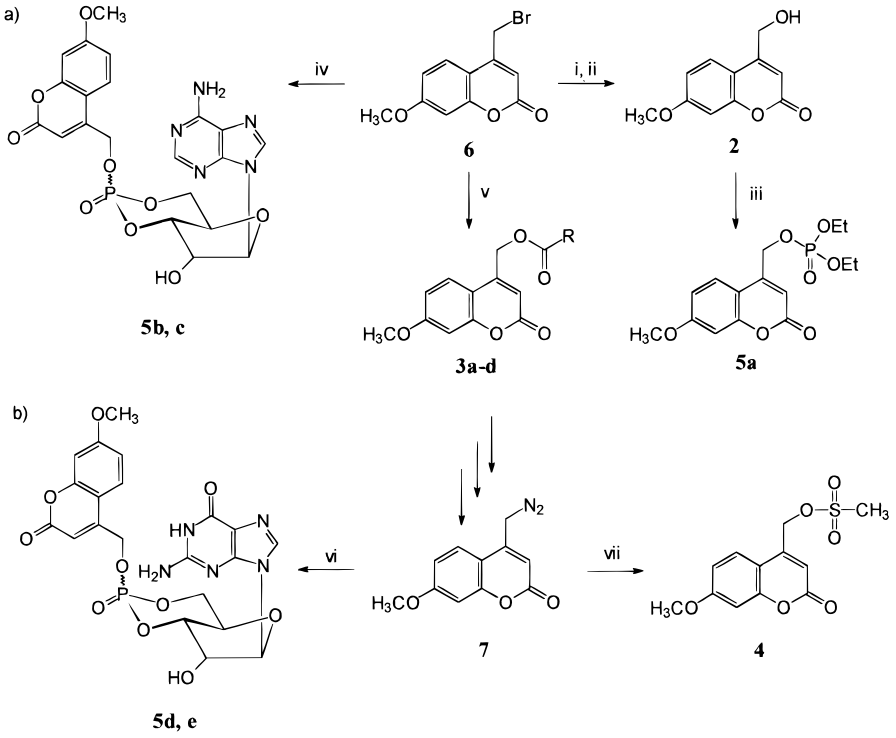

[a] Key (a) i, acetanhydride/NaOAc, reflux, 2 h; ii, HCl/EtOH, reflux, 1 h; iii, diethyl phosphoric acid chloride/pyridine, 0 °C−rt, 4 h; iv, tetra-*n*-butylammonium salt of CAMP/CH_3CN, reflux, 5 h; v, acid/acetone/KF, rt (reflux), 1 d (3 h); (b) vi, CGMP dihydrate/CH_3CN/DMSO, 50 °C, 1 d; vii, methanesulfonic acid/$CHCl_3$, rt, 2 h.

boxylic acids into their corresponding photolabile MCM esters. The synthesis procedure led to high or almost quantitative yields, respectively. Attempts to obtain MCM mesylate (**4**) via conversion of **2** with methanesulfonic acid chloride or methanesulfonic acid anhydride led to decomposition of **2**. **4** was obtained in moderate yields starting from the 4-(diazomethyl)-7-methoxycoumarin (**7**).[11] MCM diethyl phosphoric acid ester (**5a**)[12] was synthesized by reaction of diethyl phosphoric acid chloride with **2** in pyridine, adapting a procedure described by Givens for benzyl phosphates[13] (Scheme 3a).

For the synthesis of MCM-*caged* cAMP (**5b**,**c**) we used the alkylation of the tetra-*n*-butylammonium salt of cAMP with 4-(bromomethyl)-7-methoxycoumarin (**6**). This method afforded **5b,c** in relatively high yields as a mixture of diastereomers (axial **5b** and equatorial **5c**). Our synthesis procedure is superior to the silver(I) oxide method described by Iwamura et al.[14] because of better yields, a higher diastereomeric excess in favor of **5b**, and the shorter reaction time as well as easier workup. Obviously the increase of nucleophilic reactivity of the nucleotide phosphate anion by tetra-*n*-butylammonium salt formation is more effective than the Lewis acid activation by silver(I) oxide. Contrary to the synthesis of **5b,c**, attempts to obtain MCM-*caged* cGMP **5d,e** by reaction of **6** with the tetra-*n*-butylammonium salt of cGMP or by reaction of **6** with the free acid of cGMP in the presence of silver(I) oxide failed. Only traces of the target molecule were obtained. Finally the alkylation of the free acid of cGMP with **7** was successful. The diastereomeric mixtures of **5b,c** and **5d,e** were separated into the pure diastereomers by RP-HPLC on a preparative scale.

The isomeric species were assigned by ^{31}P NMR as reported for the axial and equatorial isomers of known cAMP and cGMP esters.[15] The ^{31}P NMR signals at higher field (δ −5.1) correspond to the axial isomers **5b,d** and those at lower field (δ −3.6 for **5c** and −4.0 for **5e**) to the equatorial isomers.

Ground-State and UV/Vis Spectroscopic Properties of the Photolabile Compounds. For our investigations acetonitrile/HEPES buffer and methanol/HEPES buffer solutions were used, which correspond broadly to physiological conditions. The absorption spectra of the "basic chromophore" **1** and **3a**−**5e** differ only insignificantly from each other and are characterized by two intensive absorption maxima around λ = 325 nm and λ = 217 nm (Table 1). The bathochromic shift of the long-wavelength absorption of the MCM moiety of about 15 nm compared to the unsubstituted (coumarin-4-yl)methyl system is due to the "push−pull effect" between the methoxy donor and the carbonyl acceptor. In the case of the bichromophoric systems **3b**−**d** and **5b**−**e** a third absorption band, characterized by a maximum in the region λ = 210−290 nm, is due to local excitation of the benzoic acids and purine bases, respectively. A comparison with the absorption spectra of the partial chromophores shows that the spectra of **3b**−**d** and **5b**−**e** are a superimposition of these partial spectra. The long-wavelength absorption of the MCM chromophore of all photolabile derivatives with regard to its position as well

(11) Ito, K.; Sawanobori, J. *Synth. Commun.* **1982**, *12* (9), 665−671.
(12) First described by: Givens, R. S.; Matuszewski, B. See ref 7.
(13) Givens, R. S.; Matuszewski, B.; Athey, P. S.; Stoner, M. R. *J. Am. Chem. Soc.* **1990**, *112*, 6016−6021.
(14) Furuta, T.; Torigai, H.; Osawa, T.; Iwamura, M. *J. Chem. Soc., Perkin Trans 1* **1993**, 3139−3142.
(15) (a) Engels, J. *Bioorg. Chem.* **1979**, *8*, 9−16. (b) Nerbonne, J. M.; Richard, S.; Nargeot, J.; Lester, H. A. *Nature* **1984**, *310*, 74−76.

Table 1. UV/Vis Spectroscopic Properties of the Investigated MCM Derivatives [50 μM Solutions in Acetonitrile/HEPES Buffer Solution (30/70) Except for 5b−e: 10 μM in Methanol/HEPES (20/80)]

	λ_{max}/nm	ϵ/L mol^{-1} cm^{-1}		λ_{max}/nm	ϵ/L mol^{-1} cm^{-1}
1	321	13.600	**4**	325	13.000
	218	15.900		219	15.700
2	320	13.300	**5a**	324	13.900
	219	16.000		219	15.900
3a	324	13.500	**5b**	328	13.200
	219	15.800		258	14.900
				207	34.900
3b	324	13.600	**5c**	325	13.300
	260	19.000		258	15.000
	215	24.500		208	34.000
3c	324	13.000	**5d**	327	13.300
	230	19.000		276	12.000
	222	20.900		253	15.300
				220	22.500
3d	324	13.700	**5e**	325	13.300
	241	26.600		276	11.800
				252	15.200
				209	22.300

as to its intensity is only insignificantly influenced by the "leaving groups" OX (see Table 1). There were no indications in the absorption spectra from which we could infer conjugative or other interactions (through-space, hydrogen bonds, charge transfer) within the ground state.

Mechanistic Pathway of the Photolytic Cleavage. Verification of the reaction pathway including potential intermediates and transition states is the basis for the qualitative discussion of the photophysical and -chemical data obtained. Excitation of solutions of the photolabile MCM esters **3a**−**5e** in acetonitrile/HEPES buffer solution (30/70) or methanol/HEPES buffer solution (20/80) within the long-wavelength absorption maximum with UV irradiation of 333 nm led to photochemical cleavage with release of the corresponding carboxylic acids (**3a**−**d**), methansulfonic acid (**4**), and phosphoric acids (**5a**−**e**). **2** was obtained with yields ≥95% as major product of the photolysis besides the released acids (Scheme 4a). This result is in agreement with observations made by Givens and Matuszewski[7] for the photolytic cleavage of MCM phosphates, by Furuta et al.[4] for MCM−cAMP, and by Hagen et al.[16] for MCM-*caged* 8-Br-cAMP and MCM-*caged* 8-Br-cGMP. The photochemical quantum yields Φ_{chem} of these reactions are summarized in Table 2.

To elucidate the reaction pathway of the photolytic cleavage after electronic excitation, especially in terms of a mechanistic distinction between a photo S_N1 or a photosolvolysis reaction, a solution of **5a** in acetonitrile/^{18}O labeled water (30/70) was irradiated. ESI mass spectrometric analysis of the separated reaction products showed that only photolysis product **2** contained the ^{18}O isotope; the liberated diethylphosphoric acid was not labeled (Scheme 4b). From this result we conclude that the photolytic reaction of the excited-state proceeds according to Scheme 1a under cleavage of the CH_2−OP bond, while the CH_2O−P bond remains intact (Scheme 1b). Consequently an ion pair is postulated as the decisive intermediate (Scheme 5) which undergoes a nucleophilic attack of OH^- or water, respectively (in the case of aqueous solvent mixtures), after a successful escape reaction with the solvent in competition with the recombination (k_0). As with the photolysis of other phosphoric acid esters,[13] it is not clear whether the ion pair formation proceeds directly from the S_1 state by heterolytic bond cleavage (k_1) or by homolytic cleavage followed by single electron transfer (k_{set}). However, formation of a singlet radical pair from S_1 is of minor importance, since in that case one should expect occurrence of hydrogen abstraction products derived from the escaped radicals, formed from the triplet state after intersystem crossing. However, only traces of **1** were found (≤0.5% compared to the formation of **2**). Furthermore no phosphorescence which would be characteristic for the population of any triplet states could be detected in any of the photolabile MCM derivatives nor the basic chromophors **1** and **2**. Therefore further kinetic considerations will be made on the basis of heterolytic bond cleavage from the S_1 state. On the basis of these results, we exclude a significant participation of the triplet state during photolysis contrary to Furuta and Iwamura,[23] who proposed a triplet mechanism for the photolytic cleavage of (7-methoxycoumarin-4-yl)methyl diethyl phosphate.

The S_N1 mechanism of the reaction characterized by solvent-assisted photoheterolysis (marked by the ion-pair stability) as the rate-determining step is also supported by the fact that higher values for Φ_{chem} were obtained with an increasing leaving group ability of OX (see Table 2; Φ_{chem} (**4**) > Φ_{chem} (**5a**) > Φ_{chem} (**3a**−**d**)). The ability of good leaving groups to stabilize the corresponding anion leads to an encouragement of the photoreaction which is characteristic of the S_N1 case. From the cationic view the stabilization of the coumarinylmethyl cation should benefit from the increased electron density within the aromatic system, which is given according to eq 1 by the methoxy substituent in position 7.

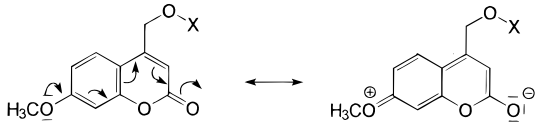

(1)

Equation 2 is valid for the photochemical quantum yield. In general, an effective photochemical cleavage is

$$\Phi_{chem} = \frac{k_1}{k_1 + k_f{}^n + k_{nr}} \cdot \frac{k_{esc}}{k_{esc} + k_0}$$

observed, if (a) the rate of competing photophysical deactivation (fluorescence and nonradiative; $k_f{}^n + k_{nr}$) is low and therefore the "physical" lifetime of the excited state is high, (b) the stability of the coumarinylmethyl cation intermediate and of the anionic product, respectively, is high, such that the rate of the ion formation (k_1) can compete successfully with the photophysical deactivation, and (c) the escape process (k_{esc}) is favored

(16) Hagen, V.; Bendig, J.; Frings, S.; Wiesner, B.; Schade, B.; Helms, S.; Lorenz, D.; Kaupp, U. B. *J. Photochem. Photobiol. B: Biol.*, in press.

(17) Dippy, J. F. J. *J. Chem. Soc.* **1938**, *9*, 1222−1227.
(18) Vandenbelt, J. M.; Henrich, C.; Vanden Berg, S. G. *Anal. Chem.* **1954**, *26*, 726.
(19) Willi, A. V.; Stocker, J. F. *Helv. Chim. Acta* **1955**, *38*, 1279.
(20) Wideqvist, B. *Ark. Kemi* **1951**, *2*, 383−386.
(21) Marziano, N. C.; Sampoli, M.; Gonizzi, M. *J. Phys. Chem.* **1986**, *90* (18), 4347−4353.
(22) Galkin, V. I.; Sayakhov, R. D.; Garifzyanov, A. R.; Cherkasov, R. A.; Pudovik, A. N. *Dokl. Chem. (Engl. Transl.)* **1991**, *318*, 114−116.
(23) Furuta, T.; Whang, S. S.-H.; Dantzker, J. L.; Dore, T. M.; Bybee, W. J.; Callaway, E. M.; Denk, W.; Tsien, R. Y. *Proc. Natl. Acad. Sci. U.S.A.* **1999**, *96*, 1193−1200 and references cited herein.

Scheme 4. Photolysis of MCM Derivatives

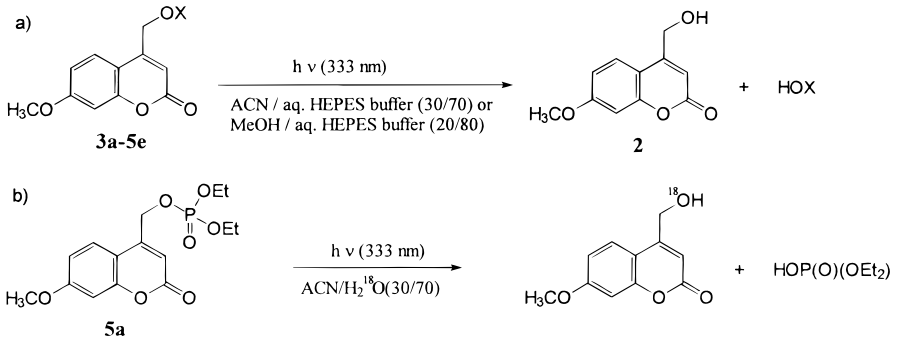

Table 2. Photophysical and Photochemical Deactivation Behavior Data of the Examined MCM Derivatives

	Φ_{chem}	Φ_f	λ_{max}^{em}/nm	Φ_{nr}	τ_f/ns	pK_a[b]	$k_f/10^9$ s^{-1}	$k_f^n/10^9$ s^{-1}	$k_{chem}/10^9$ s^{-1}	$k_{nr}/10^9$ s^{-1}
3a	0.0043	0.37	400	0.63	1.41	4.89[17]	0.71	0.26	0.0030	0.444
3b	0.0045	0.42	400	0.58		4.41[18]				
3c	0.0052	0.43	400	0.56		3.99[19]				
3d	0.0064	0.08	402	0.91		3.54[20]				
4	0.081	0.0072	394	0.91	≪0.2	−1.54[21]	≫5	0.036	0.41	4.56
5a	0.037	0.052	404	0.91	<0.2	0.71[22]	>5	0.26	0.19	4.55
5b[a]	0.13	0.030	400	0.84	≪0.2	≫5	0.15	0.65	4.20	
5c[a]	0.070	0.040	400	0.89						
5d[a]	0.21	0.014	400	0.78						
5e[a]	0.092	0.030	401	0.89						

[a] Values in methanol/(aqueous) HEPES buffer solution (20:80 v/v). [b] pK_a value of the corresponding acid.

Scheme 5. Reaction Pathway and Mechanism of the Photolytic Cleavage

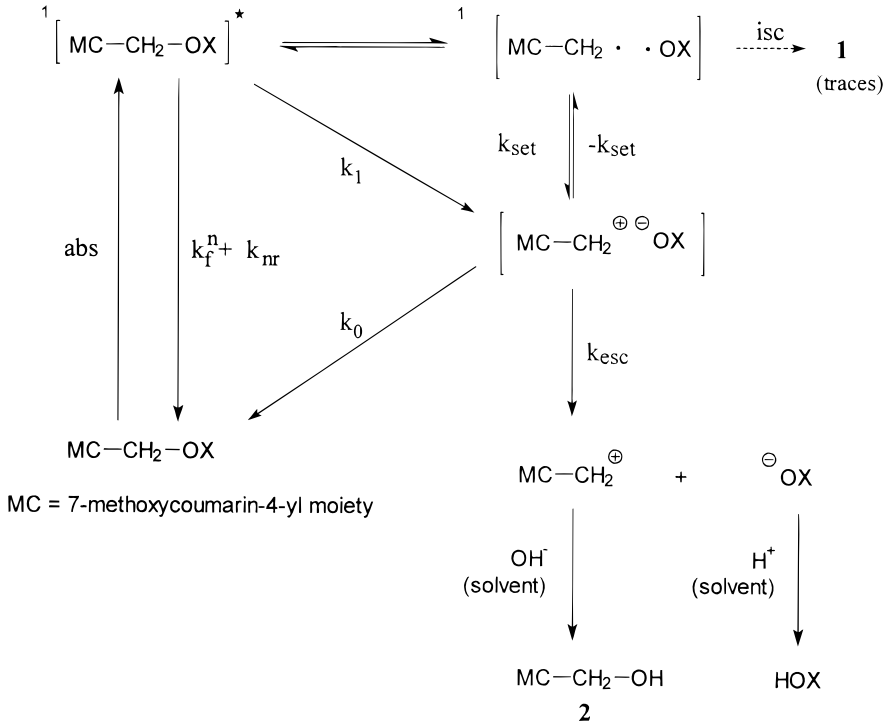

due to the stability of the solvated anions and can also compete successfully with the ion recombination (k_0 based on pseudo-internal conversion).

Photophysical Deactivation Behavior of 2. With regard to a better understanding of the fluorescence enhancement caused by the appearance of **2** during the irradiation of **4** and **5a**−**e**, we studied the photophysics of **2** in more detail. Furthermore **2** was used as a model compound in order to examine the environmental (solvent) influence on the deactivation behavior of the MCM system in general. The fluorescence emission spectrum of **2** is quite similar to those of the photolabile derivatives **3a**−**5e** with regard to the spectral position. However, there are considerable differences in the intensity of emission (more than 1 order of magnitude). **2** shows a fluorescence quantum yield Φ_f of 0.1−1 in polar protic solvents. On the other hand Φ_f is only 0.0014 in cyclohexane.[8] Also by using polar protic solvents we observed a systematic dependence of Φ_f and τ_f on the solvent polarity. It appears that the participation of fluorescence as a main deactivation process increases with the water content of the solvent mixture (Table 3). From photoacoustic measurements and from the absence of a phosphorescence spectrum at 77 K (ethanolic solution) we

Table 3. Solvent Dependence of the Photophysical Deactivation of 2

	ratio aqueous HEPES buffer solution/methanol						ratio aqueous HEPES buffer solution/acetonitrile						
x	Φ_f	Φ_{nr}	Φ_f/ns	Φ_f^n/ns	$k_f/10^9\ s^{-1}$	$k_f^n/10^9\ s^{-1}$	$k_{nr}/10^9\ s^{-1}$	Φ_f	Φ_{nr}	τ_f/ns	τ_f^n/ns	$k_f/10^9\ s^{-1}$	$k_f^n/10^9\ s^{-1}$	$k_{nr}/10^9\ s^{-1}$
0/100	0.10	0.91	0.43	4.53	2.33	0.22	2.11	0.012	0.988	<0.2	16.67	>5	0.060	4.94
20/80	0.31	0.69	0.74	2.39	1.35	0.42	0.93	0.13	0.88	0.40	3.20	2.50	0.31	2.19
40/60	0.47	0.53	1.10	2.34	0.91	0.43	0.48	0.18	0.82	0.59	3.28	1.70	0.31	1.39
60/40	0.59	0.41	1.63	2.76	0.61	0.36	0.25	0.26	0.74	0.87	3.35	1.15	0.30	0.85
70/30								0.40	0.60	1.33	3.33	0.75	0.30	0.45
80/20	0.65	0.35	2.20	3.38	0.46	0.30	0.16							
100/0								0.55	0.45	1.88	3.42	0.53	0.29	0.24
THF	0.007	0.993	≪0.2	28.57	≫5	0.035	4.97							
dioxane	0.006	0.994	≪0.2	33.33	≫5	0.030	4.97							

Scheme 6. Schematic Presentation of the Term Schemes for the Lowest Lying Excited States of 4 in (a) Nonpolar and (b) Polar Protic Solvents

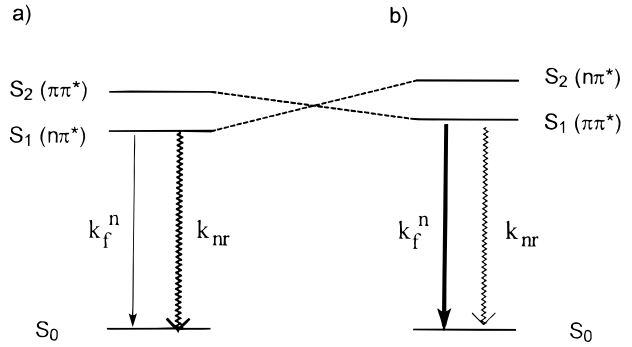

conclude that the isc process is not significant in the deactivation of the S_1 state ($\Phi_{isc} \ll 0.05$). Analysis of the rate constants for the radiative (k_f^n) and the nonradiative ($k_{nr} \approx k_{ic}$) deactivation as competing processes (see Table 3) shows that the solvent effect is mainly due to k_{nr}. Whereas k_f^n appears almost independent of the solvent, k_{nr} increases up to 1 order of magnitude within the series from water to the pure solvents acetonitrile and methanol respectively (Table 3). This behavior determines the relative positions of the S_1 ($n\pi^*$) and S_2 ($\pi\pi^*$) states in the term scheme of **2** (and the MCM chromophore in general) and derives from the solvent dependence of the distance between these energy levels. Scheme 6 presents the position of these levels for **1** which is comparable to **2** due to the isoelectronic behavior with regard to n and π electrons (for quantum mechanical considerations, see ref 8). In a nonpolar aprotic environment there is a dominating $n\pi^*$ character for S_1 despite the coupling and mixing of the S_1 and S_2 states. This results in a high probability for the nonradiative transition and therefore in a low radiative efficiency of fluorescence for the transition $S_1(n\pi^*) \rightarrow S_0$ (Scheme 6a). In the case of polar protic solvents the $S_1(n\pi^*)$ state is of higher energy and the energy of the $S_2(\pi\pi^*)$ state is reduced, which should lead to an approach or even inversion of the energy levels. Therefore the deactivation behavior of the S_1 state is characterized by a $\pi\pi^*$ state or by a state with a dominating $\pi\pi^*$ character. As a consequence, the disadvantage of the internal conversion process due to the lower vibronic coupling results in an increasing participation of fluorescence in the deactivation. The data summarized in Table 3 also illustrate this effect for aqueous solvent mixtures. Whereas the rate of fluorescence k_f^n remains nearly constant, k_{nr} decreases with increasing molar ratio of water leading to an increase of Φ_f and τ_f.

Structural and Solvent Dependencies of the Photochemical and Fluorescence Deactivation Efficiency of the *Caged* Compounds. The investigated *caged* derivatives have the same coumarinyl moiety as the chromophoric system. The absorption properties show that there is no interaction, at least in the ground state, which would significantly change the electronic system with regard to its energy and symmetry (transition probability). It can thus be concluded that in principle the rates of photophysical deactivation k_f^n and k_{ic} (estimated for **1** and **2**) are comparable for all the compounds investigated. According to eqs 3 and 4 therefore, the

$$\Phi_f = \frac{k_f^n}{k_1 + k_{nr} + k_f^n} \qquad (3)$$

$$\tau_f = \frac{1}{k_1 + k_f^n + k_{nr}} \qquad (4)$$

progressive change in Φ_f and τ_f which were found by structural variation (Table 2) must be due to the structural dependence of k_1. A high value for k_1 should occur if both the cation within the ion pair (constant in the MCM case) and the anion formed (leaving group) are stable or stabilized, respectively. The latter can be seen as the reason for the decrease of fluorescence quantum yield and therefore the increase of the efficiency of photochemistry with better leaving group ability. The pK_a values given in Table 2 describe the anion stability and accordingly represent the leaving group ability. Since the mesylate and diethyl phosphate are superior to carboxylates in this respect, the derivatives **4** and **5a** exhibit a higher photoreactivity. Figure 1 illustrates this relationship.

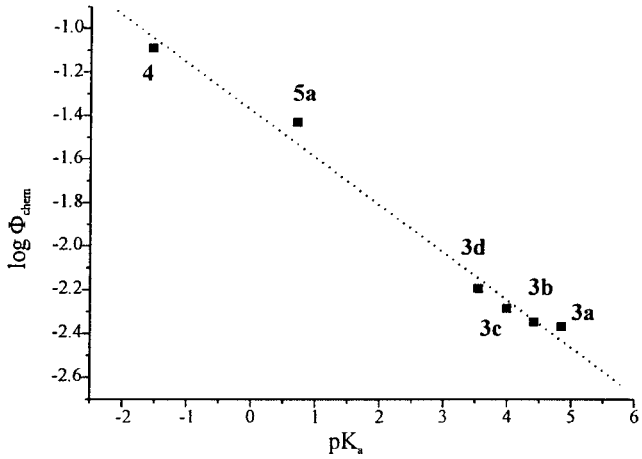

Figure 1. Relationship between photochemical quantum yield Φ_{chem}, and leaving group ability, represented by the pK_a values of the corresponding acid.

As expected, the progressive change of the electronic structure of the anion has significant effects as observed for the substituted MCM benzoic acid esters (**3b**−**d**). Thus the appearance of the electron-withdrawing cyano group at the para position of the benzoic acid ester (**3d**) leads to an increased photochemical quantum yield, whereas methoxy substitution (**3b**) leads to a decreased rate of the photoreaction. Besides the direct structural influence due to the stabilization of the leaving group, an additional structural influence of the nucleoside moiety can be observed for the phosphoric acid esters **5b**−**e**. Both compounds show an increased photochemical quantum yield compared to the diethyl phosphate **5a**. This effect can be explained by additional stabilization of the MCM cation (by partial charge transfer) and/or the anion (by hydrogen bonding) within the ion pair intermediate by the purine base, respectively. The question as to what extent an exciplex interaction between the purine base and the coumarinyl moiety occurs as an element of this stabilization within the excited S_1 state[24] cannot be answered. On the basis of the differences concerning the donor ability of adenine and guanine, the stabilization of the intermediate is greater for the cGMP compared to the corresponding cAMP derivatives, as reflected by higher values for the photochemical quantum yield. Thus the one electron standard oxidation potential $E°(N^{•+}/N)$ in acetonitrile has values of 1.47 V (guanosine) and 1.94 V (adenosine), respectively.[24]

Furthermore a small but significant difference is observed by comparison of the deactivation parameters for the diastereomers (Table 2). Due to steric reasons an interaction between the purine base and the positively charged center should be favored within the axial configuration. As a result of the competing processes of photochemistry and fluorescence, the axial isomers **5b**,**d** show higher photochemical quantum yields, whereas a stronger fluorescence is observed for the equatorial isomers **5c**,**e**.

As in the case of **2** the photophysical and photochemical deactivation behavior of the *caged* compounds is strongly dependent on the solvent and the composition of the solvent mixtures. Thus the efficiency of the photoreaction increases continuously with increasing amount of the stronger polar protic solvent component whereas the fluorescence quantum yield increases at the beginning and decreases after reaching a maximum during the same solvent variation. Figure 2 represents this effect for the diethyl phosphate **5a**. A very similar behavior was observed for the photolabile MCM derivatives **3**, **4**, and **5b**−**e**. The interpretation of the increase of Φ_{chem} is given by the opportunity of better stabilization of the ion pair by solvation which leads to an acceleration of k_1 and, therefore, according to eq 2 to the consequent continuous increase of Φ_{chem}. Additionally the polarity dependence of the rate of photolysis is further evidence for the S_N1 character of the photolytic cleavage. With regard to the solvent dependence of the fluorescence quantum yield there is a superimposition of two opposing effects: first, the solvent dependent rate of nonradiative deactivation ($k_{ic} \approx k_{nr}$) which *decreases* with increasing polarity and, second, the rate of the photochemical reaction k_1 which *increases* with increasing polarity. The fluorescence quantum yield Φ_f is described by eq 3. Therefore the

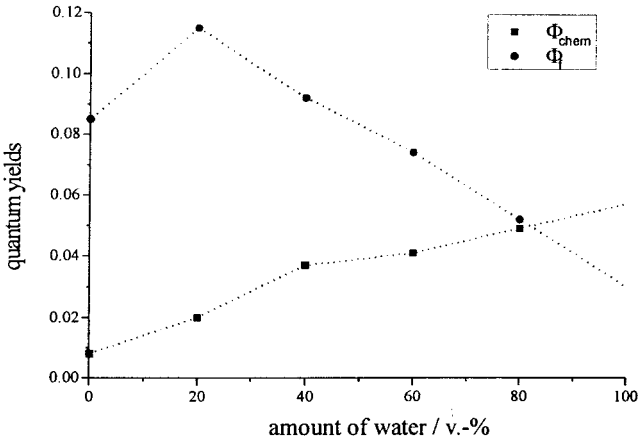

Figure 2. Competition between photophysical (Φ_f) and photochemical ($\Phi_{chemical}$) deactivation as a function of the polarity of the aqueous solvent mixture for **5a**.

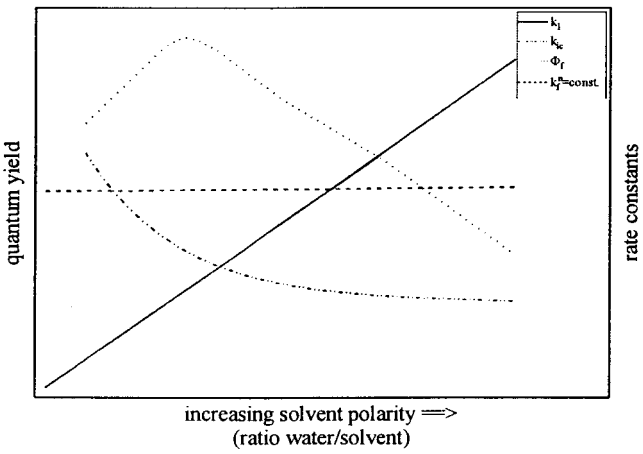

Figure 3. Schematic relationship between the kinetic data for the deactivation of excited MCM derivatives and increasing solvent polarity.

global effect is the result of the initially dominating decrease of $k_{ic} \approx k_{nr}$ from the less polar solvent composition. This effect becomes overcompensated progressively by the contrary dependence of k_1 on the solvent polarity. That relationship is schematically illustrated in Figure 3.

In conclusion, MCM esters liberate the corresponding acids during photolysis and are suited for the creation of *caged* compounds and therefore for the triggering of potential biologically active molecules with such functional groups. As we could show, this liberation proceeds in the nanosecond time region, confirming the usefulness of the MCM moiety as a *caging* group. A strong polarity of the solvent favors the rate of photolysis. Analysis of the photolytic products and of the kinetic data as well as the results of isotope labeling studies show that the reaction proceeds via a photo S_N1 mechanism (solvent-assisted photoheterolysis), with formation of an ion pair as intermediate. Mechanistically determined, the photocleavage is most effective in the case of good leaving groups such as sulfonic and phosphoric acid derivatives. In these cases the photolytic liberation is combined with a marked fluorescence enhancement which should be suited for the visualization of the uncaging process inside living cells. With regard to the fluorescence enhancement

(24) Seidel, C. A. M.; Schulz, A.; Sauer, M. H. M. *J. Phys. Chem.* **1996**, *100*, 5541−5553.

and kinetics of photocleavage the MCM system is at the limits of its efficiency in the case of phosphates and sulfonates.

Further studies with regard to the influence of the type and position of substituents on the coumarinyl moiety on the "cationic stabilization" of the *caged* derivatives are in progress.

Experimental Section

Materials and General Methods. 7-Methoxy-4-methylcoumarin and 4-(bromomethyl)-7-methoxycoumarin were purchased from Sigma (Germany). 4-(Diazomethyl)-7-methoxycoumarin (**7**) was synthesized according to Ito[25] starting with selective oxidation of **1** to the carbaldehyde, subsequent formation of the tosylhydrazone, and cleavage with triethylamine to the diazo compound. TLC plates, silica 60-F_{254}, were from E. Merck (Darmstadt, Germany). Silica gel (30−60 μm) for flash chromatography was purchased from J. T. Baker (The Netherlands). Acetonitrile from Riedel-deHaën (Germany) was HPLC grade. All other chemicals and solvents were reagent grade and were used without further purification. Water was purified with a Milli Q system (Millipore, Germany). Analytical HPLC was run on a Hewlett-Packard HP 1100 system with DAD and fluorescence detection; for preparative HPLC a Shimadzu LC-8A system with UV detection (SPD-6AV) was used. A C_{18} column (Spherisorb ODS 2, 5 μ, 250 × 4 mm, Polymer Laboratories Ltd., U.K.) was used for HPLC analysis at a flow rate of 1 mL/min at 20 °C with an injection volume of 20 μL. Preparative HPLC was run using a Nucleosil 100−7 C_{18} column (7 μ, 250 × 20 mm, Machery-Nagel, Germany) at a flow rate of 10 mL/min. Eluent A was water, and eluent B acetonitrile. ^{1}H NMR and ^{13}C NMR were recorded on a Gemini 200 spectrometer (Varian) using TMS as internal standard. ^{31}P NMR spectra were recorded using a Bruker DRX 600 spectrometer with 85% phosphoric acid as external standard. All melting points are uncorrected.

Syntheses. (7-Methoxycoumarin-4-yl)methyl-*n*-heptanoate (3a). To a suspension of 283 mg (1.05 mmol) of **6** in 20 mL of acetone were added 122 mg (2.1 mmol) of potassium fluoride and 137 mg (1.05 mmol) of *n*-heptanoic acid. The mixture was stirred at room temperature for 1 d, and then the solvent was removed in vacuo. The residue was suspended in 20 mL water and extracted with 2 × 40 mL of ethyl acetate. The combined organic phases were dried with sodium sulfate, and the solvent was evaporated in a vacuum. Flash chromatography of the residue with petroleum ether/ethyl acetate (8:2 v/v) yielded 279 mg (0.876 mmol; 82.6%) of **3a** as a pale yellow solid: mp 94 °C; ^{1}H NMR ($CDCl_3$) δ 0.89 (3H, t, J = 6 Hz), 1.27−1.36 (8H, m), 2.46 (2H, t, J = 7.5 Hz), 3.90 (3H, s), 5.31 (2H, s, 6.35 (1H, s), 6.87−6.89 (2H, m), 7.42−7.44 (1H, m); EI mass spectrum *m/e* (relative intensity) 319 (M^+ + 1, 4), 318 (M^+, 16), 189 (6), 175 (2), 129 (2), 85 (33). Anal. Calcd for $C_{18}H_{22}O_5$: C, 67.91; H, 6.97. Found: C, 67.8; H, 6.97.

(7-Methoxycoumarin-4-yl)methyl-4-methoxybenzoate (3b). This was made analogously to **3a** using 465 mg (1.68 mmol) of **6**, 215 mg (1.41 mmol) of 4-methoxybenzoic acid, and 204 mg (3.51 mmol) of potassium fluoride in 20 mL acetone. Yield: 432 mg (1.38 mmol; 90.0%) of **3b** as a pale yellow solid, mp 158 °C. ^{1}H NMR ($CDCl_3$): δ 3.88 (6H, s), 5.47 (2H, s), 6.43 (1H, s), 6.85−6.98 (4H, m), 7.47−7.51 (1H, m), 8.04−8.08 (2H, m). ^{13}C NMR ($CDCl_3$): δ 56.0, 56.3, 61.9, 101.8, 110.4, 111.2, 113.2, 114.4 (2C), 121.8, 125.0, 132.4 (2C), 150.1, 156.1, 161.5, 163.4, 164.5, 165.9. ESI mass spectrum: *m/e* 341.2 [M + H]$^+$. Anal. Calcd for $C_{19}H_{16}O_6$: C, 67.05; H, 4.74. Found: C, 67.16; H, 4.86.

(7-Methoxycoumarin-4-yl)methylbenzoate (3c). Analogously to **3a** a mixture of 510 mg (1.90 mmol) of **6**, 287 mg (2.35 mmol) of benzoic acid, and 237 mg (4.08 mmol) of potassium fluoride was refluxed in 20 mL of acetone for 3 h. The resulting mixture was suspended in 20 mL of water and extracted with 2 × 40 mL of ethyl acetate. The combined organic phases were dried with sodium sulfate, and the solvent was evaporated in a vacuum. Flash chromatography of the residue through a short column with chloroform yielded 576 mg (1.86 mmol; 98%) of **3c** as a pale yellow solid, mp 151 °C: ^{1}H NMR ($CDCl_3$) δ 3.88 (3H, s), 5.50 (2H, s), 6.44 (1H, s), 6.86−6.91 (2H, m), 7.44−7.62 (4H, m), 8.84−8.12 (2H, m); ^{13}C NMR ($CDCl_3$) δ 56.5, 62.3, 101.9, 110.6, 111.3, 113.3, 125.1, 129.3 (2C), 129.6, 130.5 (2C), 134.4, 150.0, 156.2, 161.5, 163.6, 166.3; ESI mass spectrum *m/e* 311.2 [M + H]$^+$. Anal. Calcd for $C_{18}H_{14}O_5$: C, 69.67; H, 4.55. Found: C, 69.62; H, 4.52.

(7-Methoxycoumarin-4-yl)methyl-4-cyanobenzoate (3d). This was made analogously to **3c** using 517 mg (1.92 mmol) of **6**, 423 mg (2.88 mmol) of 4-cyanobenzoic acid, and 277 mg (4.77 mmol) of potassium fluoride in 20 mL of acetone. After 3 h of reflux acetone was evaporated; the residue was suspended in chloroform and washed with diluted sodium chloride solution. The organic phase was washed with $NaHCO_3$ in order to remove unconverted 4-cyanobenzoic acid. After neutralization the solvent was evaporated. Yield: 540 mg (1.61 mmol; 83.8%) of **3d** as a yellow solid. The crude product was further purified by preparative HPLC using a linear gradient 5−80% B in 45 min; t_R = 43 min (λ_{Det} = 320 nm) followed by lyophilization: mp 243 °C; ^{1}H NMR ($CDCl_3$) δ 3.90 (3H, s), 5.55 (2H, s), 6.41 (1H, s), 6.88−6.94 (2H, m), 7.46−7.51 (1H, m), 7.78−7.82 (2H, m), 8.19−8.24 (2H, m); ^{13}C NMR ($CDCl_3$) δ 56.5, 63.0, 102.0, 111.0, 111.2, 113.6, 117.9, 118.4, 125.8, 129.0 (2C), 133.3 (2C), 133.5, 149.2, 156.4, 161.4, 163.8, 164.8; ESI mass spectrum *m/e* 336.3 [M + H]$^+$. Anal. Calcd for $C_{19}H_{13}O_5$: C, 68.06; H, 3.91; N, 4.18. Found: C, 68.12; H, 3.98, N, 4.22.

(7-Methoxycoumarin-4-yl)methylmethanesulfonate (4). To a suspension of 474 mg (2.19 mmol) of **3** in 10 mL of chloroform was added 277 mg (2.88 mmol) of methanesulfonic acid in 1 mL of chloroform dropwise under vigorous stirring at room temperature. The mixture was refluxed for 3 h. Evaporation of the solvent and recrystallization of the residue from THF yielded 162 mg (0.57 mmol, 26%) of **11** as a pale yellow solid. The compound was further purified by preparative HPLC using a linear gradient 5−50% B in 45 min, isocratic 50% B from 45 to 50 min; t_R = 45 min (λ_{Det} = 320 nm) followed by lyophilization: mp 159 °C; ^{1}H NMR (DMSO-d_6) δ 3.37 (3H, s), 3.87 (3H, s), 5.54 (2H, s), 6.38 (1H, s), 7.03−7.05 (2H, m), 7.62−7.67 (1H, m); ^{13}C NMR (DMSO-d_6) δ 39.0, 56.3, 66.9, 101.3, 110.2, 110.3, 112.7, 126.2, 149.0, 155.3, 160.1, 163.0; ESI mass spectrum *m/e* 285.1 [M + H]$^+$. Anal. Calcd for $C_{12}H_{12}O_6S$: C, 50.70; H, 4.25. Found: C, 50.65; H, 4.35.

(7-Methoxycoumarin-4-yl)methyl(diethyl)phosphate (5a). A 1.031 g (5.0 mmol) amount of **2** was suspended in 9 mL of pyridine and cooled to 0 °C. Under vigorous stirring 1.035 g (6.0 mmol) of diethylphosphoric acid chloride was added dropwise. After being stirred at 0 °C for 2 h, the mixture was allowed to warm to room temperature under continued stirring for 2 h. Water was added to dissolve precipitated pyridinium chloride. The mixture was extracted with ether (4 times), and the organic layer was washed with 2 × 10 mL of 1 N H_2SO_4, 10 mL of $NaHCO_3$ (5%), 3 × 10 mL of water, and 10 mL of brine. The combined organic phases were dried over $MgSO_4$ and evaporated. The residue was dissolved in a small amount of ether, and pentane was added. After refrigeration overnight, 1.34 g (3.91 mmol; 78.2%) of **5a** was obtained as a white solid, mp 65 °C: ESI mass spectrum *m/e* 343.1 [M + H]$^+$. NMR data are in agreement with ref 14.

(7-Methoxycoumarin-4-yl)methyl Adenosine Cyclic-3′, 5′-monophosphate (5b,c). A mixture of 323 mg (1.2 mmol) of **6** and 243 mg of the dihydrate of the tetra-*n*-butylammonium salt of cAMP (prepared from cAMP by passing through an acidic Dowex ion-exchange column equilibrated with a solution of tetra-*n*-butylammonium hydroxide followed by lyophilization) was refluxed in 30 mL of acetonitrile in the dark for 5 h. After evaporation of the solvent the residue was washed with 20 mL of water, dried, dissolved in a small volume of chloroform/methanol (1:1 v/v), and purified by flash chromatography. Elution using chloroform removed unconverted **6** from the column. Elution with chloroform/methanol (2.5:97.5

(25) Ito, K.; Maruyama, J. *Chem. Pharm. Bull.* **1983**, *31* (9), 3014−3023.

to 5:95 v/v) yielded 133 mg (64.4%) of the pure diastereomeric mixture of **5b,c** in a 80:20 ratio (axial/equatorial) as a colorless solid after evaporation and lyophilization. The isomers were separated from each other by preparative HPLC using a linear gradient 10−45% B in 105 min (λ_{Det} = 320 nm) followed by lyophilization.

5b: ^{1}H NMR (DMSO-d_6) δ 3.86 (3H, s), 4.29 (1H, dt, J = 10.2 and 4.8 Hz), 4.46 (1H, t, J = 9.8 Hz), 4.68−4.73 (2H, m), 5.38 (1H, dd, J = 9.8 and 5.0 Hz), 5.48 (2H, d, J = 6.3 Hz), 6.06 (1H, s), 6.43 (1H, s), 6.46 (1H, s), 6.96 (1H, dd, J = 8.8 and 2.5 Hz), 7.08 (1H, d, J = 2.4 Hz), 7.40 (2H, s br), 7.72 (1H, d, J = 8.9 Hz), 8.10 (1H, s), 8.35 (1H, s); ^{31}P NMR (DMSO-d_6) δ −5.1; ESI mass spectrum *m/e* 518.3 $[M + H]^+$.

5c: ^{1}H NMR (DMSO-d_6) δ 3.87 (3H, s), 4.51 (2H, m), 4.71 (1H, d, J = 4.7 Hz), 4.76 (1H, d, J = 12.4 Hz), 5.37 (1H, m), 5.41 (2H, m), 6.08 (1H, s), 6.39 (1H, s), 6.39−6.50 (1H, s br), 7.01 (1H, d, J = 8.8 Hz), 7.07 (1H, s), 7.40 (2H, s br), 7.69 (1H, d, J = 8.8 Hz), 8.19 (1H, s), 8.40 (1H, s); ^{31}P NMR (DMSO-d_6) δ −3.6; ESI mass spectrum *m/e* 518.3 $[M + H]^+$.

(7-Methoxycoumarin-4-yl)methyl Guanosine Cyclic-3′,5′-monophosphate (5d,e). A mixture of 191 mg (0.5 mmol) of cGMP dihydrate and 216 mg (1.0 mmol) of **7** was stirred in 20 mL of DMSO and 20 mL of acetonitrile at 50 °C in the dark for 24 h. Acetonitrile was evaporated under reduced pressure, and DMSO was removed by repeated extraction with ether. The residue was purified by flash chromatography. Elution with methanol/chloroform (1:19 to 1:4 v/v) yielded 65 mg (22.8%) of the pure diastereomeric mixture of **5d,e** in a 50:50 ratio as a colorless solid after evaporation and lyophilization. Preparative HPLC permitted complete separation into the diastereomers **d** and **e** using a linear gradient 5−45% B in 105 min (λ_{Det} = 320 nm) followed by lyophilization.

5d: ^{1}H NMR (DMSO-d_6) δ 3.86 (3H, s), 4.23 (1H, dt, J = 10.3 and 4.9 Hz), 4.55 (1H, t, J = 9.8 Hz), 4.58 (1H, t, J = 4.8 Hz), 4.68 (1H, ddd, J = 22.1, 9.3 and 4.8 Hz), 4.83 (1H, dd, J = 9.8 and 5.0 Hz), 5.45 (2H, d, J = 6.1 Hz), 5.84 (1H, s), 6.38 (1H, d, J = 4.9 Hz), 6.49 (1H, s), 6.53 (2H, s br), 6.97 (1H, dd, J = 8.9 and 2.5 Hz), 7.06 (1H, d, J = 2.4 Hz), 7.72 (1H, d, J = 8.9 Hz), 7.94 (1H, s), 10.72 (1H, s br); ^{31}P NMR (DMSO-d_6) δ −5.1; ESI mass spectrum *m/e* 534.3 $[M + H]^+$. Anal. Calcd for $C_{21}H_{20}N_5O_{10}P\cdot 2H_2O$: C, 44.30; H, 4.25; N, 12.30. Found: C, 44.30; H, 4.08; N, 11.42.

5e: ^{1}H NMR (DMSO-d_6) δ 3.87 (3H, s), 4.43−4.46 (1H, m), 4.48 (1H, m), 4.58 (1H, t, J = 4.7 Hz), 4.72−4.76 (1H, m), 5.18 (1H, dd, J = 9.4 and 5.0 Hz), 5.41 (2H, m), 5.85 (1H, s), 6.31 (1H, d, J = 4.5 Hz), 6.39 (1H, s), 6.60 (2H, s br), 7.00 (1H, dd, J = 8.9 and 2.5 Hz), 7.07 (1H, d, J = 2.4 Hz), 7.68 (1H, d, J = 8.9 Hz), 10.74 (1H, s); ^{31}P NMR (DMSO-d_6) δ −4.0; ESI mass spectrum *m/e* 534.3 $[M + H]^+$. Anal. Calcd for $C_{21}H_{20}N_5O_{10}P\cdot H_2O$: C, 45.74; H, 4.02; N, 12.70. Found: C, 45.88; H, 3.99; N, 11.79.

Steady-State UV/Vis Spectroscopy, Photolysis Experiments, and Measurements of the Photochemical Quantum Yields. UV/vis spectra were recorded with a U-3410 spectrophotometer (Hitachi, Japan). Photolysis was carried out using a high-pressure mercury lamp (HBO 500, Oriel) with controlled light intensity and a metal interference filter of 333 nm (Schott, Germany). For quantum yield determinations the irradiated solutions were analyzed using HPLC. The 20 μM solutions of the MCM-*caged* compounds in aqueous HEPES buffer solution (0.01 M HEPES/NaOH, 0.12 M NaCl, 3 mM KCl, 1 mM $CaCl_2$, 1 mM $MgCl_2$, pH 7.2)/30% acetonitrile or 20% methanol, respectively, were placed in quartz cuvettes with a path length of 1 cm and irradiated for periods ranging from 3 to 90 s in steps of 3−10 s. Before and after each irradiation absorption spectra were recorded and concentrations of the remaining *caged* compounds were measured by HPLC. The photochemical quantum yields, Φ_{chem}, defined as the ratio of *caged* molecules converted to the amount of photons absorbed, were determined as described[2b] using potassium ferrioxalate actinometry[26] according to the equation $\Phi_{chem} = (dc/dt)I_{abs}^{-1}V$. The initial slope dc/dt of the experimentally obtained concentration/irradiation time function was determined directly using the HPLC peak areas of the *caged* compounds. The value of I_{abs} (absorbed light intensity at $t = 0$ and α = 333 nm in "mol of photons" s^{-1}) was calculated using the absorption factor α (taken from the UV spectra at $t = 0$ and α = 333 nm) multiplied by the light intensity of the HBO 500 exposure tool (determined using the actinometer compound). The volume V of solution irradiated was 3 mL.

Fluorescence Measurements. Fluorescence spectra were measured using a MPF-2A fluorescence spectrometer (Hitachi-Perkin-Elmer) combined with a correction and digitalization unit. The 10 μM solutions of the compounds under investigation were placed in quartz cuvettes with a path length of 1 cm and excited in a perpendicular arrangement. In the case of the highly reactive compounds **4** and **5a**−**e**, the excitation intensity (controlled by the excitation slit) was very low and the registration time was very short (10 s) to prevent excessive photolysis.

The fluorescence quantum yields were determined at 298 K by the relative method[27] using quinine sulfate as a standard (Φ_f = 0.545 in 0.1 N H_2SO_4). At excitation wavelength (328−335 nm) the absorbance values of the solutions of the standard and the investigated compound were identical. The different refractive indices of the solutions were taken into account.

The time-resolved fluorescence decay measurements (pulse sampling method) were performed using a nitrogen laser (λ = 337 nm) as excitation source and a transient recorder for the decay registration. The wavelength of the fluorescence detection was λ_{em} = 405 nm (interference filter). Details of the equipment and the deconvolution procedure of the experimental decay curve are described in ref 28.[28] The time resolution achieved was about 250 ps.

Electrospray Mass Spectrometry. ESI mass spectrometry was performed on a triple quadrupole instrument (TSQ 700, Finnigan MAT, Germany) equipped with an electrospray ion source (API-ESI) operating in the positive mode with a capillary temperature of 200 °C and a voltage of 4.5 kV. The sample concentration was 150 pmol/μL in acetonitrile/acetic acid (99:1, v/v). The samples were introduced into the ion source at a constant flow rate of 3 μL/min. Nitrogen was used as sheath gas at a pressure of 3.4 bar. The spectra represent an average sum of 64 scans.

Acknowledgment. We thank S. Helm, B. Gentsch, and J. Lossmann for technical assistance. We are grateful to Dr. R. Winter for NMR investigations. The authors thank the Forschungsinstitut Jülich GmbH, the Deutsche Forschungsgemeinschaft (DFG), and the Fonds der chemischen Industrie for financial support.

JO9910233

(26) Kuhn, H. J.; Braslawsky, S. E.; Schmidt, R. *Pure Appl. Chem.* **1989**, *61*, 187−210.

(27) Demas, J. N.; Crosby, G. A. *J. Phys. Chem.* **1971**, *75*, 991; *EPA Newsl.* **1986**, *28*, 21.

(28) Grewer, C.; Brauer, H.-D. *J. Phys. Chem.* **1993**, *97*, 5001−5006.